Available online at www.sciencedirect.com
ScienceDirect
Journal of Catalysis 250 (2007) 342–349
JOURNAL OF CATALYSIS
www.elsevier.com/locate/jcat

Sustainable production of acrolein: Gas-phase dehydration of glycerol over Nb_2O_5 catalyst

Song-Hai Chai, Hao-Peng Wang, Yu Liang, Bo-Qing Xu *

Innovative Catalysis Program, Key Lab of Organic Optoelectronics & Molecular Engineering, Department of Chemistry, Tsinghua University, Beijing 100084, PR China

Received 28 February 2007; revised 10 May 2007; accepted 13 June 2007

Available online 6 August 2007

Abstract

Gas-phase dehydration of glycerol to produce acrolein was investigated at 315 °C over Nb_2O_5 catalysts calcined in the temperature range of 350–700 °C. The catalysts were characterized by nitrogen physisorption, TG-DTA, XRD, and n-butylamine titration using Hammett indicators to gain insight into the effect of calcination temperature on catalyst texture, crystal structure, and acidity. Calcination at 350 and 400 °C produced amorphous Nb_2O_5 catalysts that exhibit significantly higher fractions of strong acid sites at $-8.2 \leqslant H_0 \leqslant -3.0$ (H_0 being the Hammett acidity function) than the crystallized Nb_2O_5 samples obtained by calcination at or above 500 °C. Glycerol conversion and acrolein selectivity of the Nb_2O_5 catalysts were dependent of the fraction of strong acid sites ($-8.2 \leqslant H_0 \leqslant -3.0$). The amorphous catalyst prepared by the calcination at 400 °C, having the highest fraction of acid sites at $-8.2 \leqslant H_0 \leqslant -3.0$, showed the highest mass specific activity and acrolein selectivity (51 mol%). The other samples, having a higher fraction of either stronger ($H_0 \leqslant -8.2$) or weaker acid sites ($-3.0 \leqslant H_0 \leqslant 6.8$), were less effective for glycerol dehydration and formation of the desired acrolein.

Keywords: Niobium oxide (Nb_2O_5); Solid acid; Glycerol (glycerin); Acrolein; Alcohol dehydration; Sustainable technology

1. Introduction

The use of renewable resources, such as biomass, as feedstock for the production of fuels and chemicals has become an increasingly important focus in energy-related catalysis, because fossil resources will be exhausted in a few decades [1–4]. Glycerol is a main byproduct in natural triglyceride methanolysis for biodiesel production. In recent years, the increasing use and production of biodiesel has resulted in an increase of glycerol production and a price decline, which makes glycerol a particularly attractive molecule (building block) for the synthesis of other valuable chemical products [5–8]. Catalytic conversion of glycerol to acrolein by a double-dehydration reaction (Fig. 1) could be an important route for using glycerol resources and could offer a sustainable alternative to the present acrolein technology based on propylene. Various solid acid catalysts, including sulfates, phosphates, zeolites, and solid phosphoric acid (SPA), have been tested for the dehydration of glycerol in either gaseous or liquid phases [9–11]. The dehydration of glycerol also has been investigated in sub-supercritical and supercritical water (250–390 °C and 25–35 MPa) in the presence of low concentrations of liquid acids or salts [12–14]. Glycerol is usually produced as a mixture with water. The direct use of glycerol in water is advantageous over pure glycerol for the production of acrolein, but a highly water-tolerant solid acid catalyst would be developed for the purpose.

Niobium oxide (Nb_2O_5) has been used as a water-tolerant solid acid catalyst for various water-involving reactions, such as esterification, hydrolysis, dehydration, and hydration [15–18]. A key to the acidic and catalytic properties of Nb_2O_5 is its calcination or pretreatment temperature [19]. In this paper we report our investigation into the catalytic behavior of Nb_2O_5 catalysts prepared by varying the calcination temperature of a hydrated niobium oxide ($Nb_2O_5 \cdot nH_2O$) for the gas-phase dehydration of aqueous glycerol. Our data provide a basis for correlating the catalyst acidity with the catalytic performance in glycerol dehydration.

* Corresponding author. Fax: +86 10 62792122.
E-mail address: bqxu@mail.tsinghua.edu.cn (B.-Q. Xu).

0021-9517/$ – see front matter © 2007 Elsevier Inc. All rights reserved.
doi:10.1016/j.jcat.2007.06.016

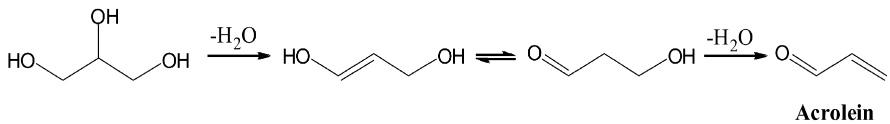

Fig. 1. Schematic representation of the double dehydration of glycerol to acrolein.

2. Experimental

2.1. Catalyst preparation

Nb_2O_5 catalysts were prepared by calcination of a hydrous niobium oxide ($Nb_2O_5 \cdot nH_2O$), provided as a HY-340 product from CBMM (Brazil). The calcination was done under flowing air (80 ml min^{-1}) in a horizontal tubular oven (50 mm i.d.) using 3.0 g of $Nb_2O_5 \cdot nH_2O$ dispersed in a quartz boat (ca. 15 ml) placed in the middle of the oven. The heating rate was 10 °C/min, and the calcination continued for 4 h at each of the selected temperatures (350–700 °C). The catalyst powders were pressed, crushed, and sieved to 20–40 mesh before use.

2.2. Characterizations

BET surface areas, pore volumes, and average pore diameters of Nb_2O_5 samples were derived from the nitrogen adsorption–desorption isotherms at −196 °C measured on a Micromeritics ASAP 2010C instrument. The samples were dehydrated under vacuum at 200 °C for 5 h before the measurement. The average pore diameter data were calculated according to the Barrett–Joyner–Halenda (BJH) method.

The crystal structures of Nb_2O_5 samples were characterized by powder X-ray diffraction (XRD) using a Bruker D8 Advance X-ray diffractometer with a Ni-filtered CuK_α ($\lambda = 0.15406$ nm) radiation source at 40 kV and 40 mA.

Thermal analysis (TG-DTA) of $Nb_2O_5 \cdot nH_2O$, as well as temperature-programmed oxidation (TPO) measurements of the used catalysts, were conducted on a Mettler-Toledo TG/SDTA 851 thermal analyzer. The sample was placed in an α-Al_2O_3 cumber and heated in flowing air (50 ml min^{-1}) from room temperature to 800 °C at a rate of 20 °C min^{-1}.

The atomic H:C ratio in the carbon deposits was determined by elemental analysis using an EAI CE-440 elemental analyzer. The samples were dried overnight at 110 °C before the measurements.

Measurements of catalyst acidity (acid strength and amount) were based on the n-butylamine titration method using various Hammett indicators, including anthraquinone ($pK_a = -8.2$), dicinnamalacetone ($pK_a = -3.0$), and neutral red ($pK_a = 6.8$), as described previously [19–21]. Acid strength was expressed by Hammett acidity function (H_0) that was scaled by pK_a values of the indicators. Before the measurement, the samples were formulated to 100–180 mesh and pretreated at 315 °C for 4 h in flowing dry N_2.

2.3. Catalytic reaction

The gas-phase dehydration of glycerol was conducted at 315 °C under atmospheric pressure in a vertical fixed-bed quartz reactor (9 mm i.d.) using 0.63 ml of catalyst. The catalyst mass in the reactor varied with the catalyst calcination temperature (T) and were 0.56 g ($T = 350$ °C), 0.57 g (400 °C), 0.61 g (500 °C), 0.73 g (600 °C), and 0.84 g (700 °C). Before the reaction, the catalysts were pretreated at 315 °C for 1.5 h in flowing dry N_2 (30 ml min^{-1}). The reaction feed, an aqueous solution containing 36.2 wt% glycerol (molar ratio glycerol/water = 1/9), was fed into the reactor by a micro-pump at a space velocity (GHSV) of glycerol of 80 h^{-1}. The reaction products were condensed in an ice–water trap and collected hourly for analysis on a HP6890 gas chromatograph equipped with a HiCap CBP20-S25-050 (Shimadzu) capillary column (0.32 mm i.d., 25 m long) and a flame ionization detector. The reaction was usually conducted for 10 h, and the condensed products during the first hour of the reaction were abandoned due to poor material balance. Conversion of glycerol (GL) and product selectivity were obtained according to the following calculations:

$$\text{GL conversion (\%)} = \frac{\text{moles of GL reacted}}{\text{moles of GL in the feed}} \times 100$$

and

$$\text{product selectivity (mol\%)} = \frac{\text{moles of carbon in a product defined}}{\text{moles of carbon in GL reacted}} \times 100.$$

3. Results

3.1. Nitrogen physisorption

Fig. 2 shows the nitrogen physisorption isotherms of the calcined Nb_2O_5 samples. None of these isotherms falls into the six types of physisorption isotherms defined by IUPAC; hysteresis loops were observed, which are usually associated with capillary condensation in mesopores [22]. For the samples calcined at 350, 400, and 500 °C, the hysteresis loops at relative nitrogen pressure (P/P_0) below 0.85 resembled type H2, but those at higher pressures were similar to type H3. Nb_2O_5 samples calcined at 600 and 700 °C also displayed type H3 hysteresis loops at $P/P_0 > 0.80$. The type H2 hysteresis loop, associated with materials with complex interconnected networks of pores of different sizes and shapes, is usually taken as the indication for the presence of pores with narrow mouths (i.e., ink bottle pores) or channel-like pores of relatively uniform size [22]. The type H3 loop characterizes slit-shaped pores formed from aggregates of plate-like particles [22].

Textural properties of the Nb_2O_5 samples derived from the nitrogen physisorption isotherms are given in Table 1. Increasing the calcination temperature resulted in continuous decreases in the sample surface area (from 115 to 7 $m^2 g^{-1}$) and pore

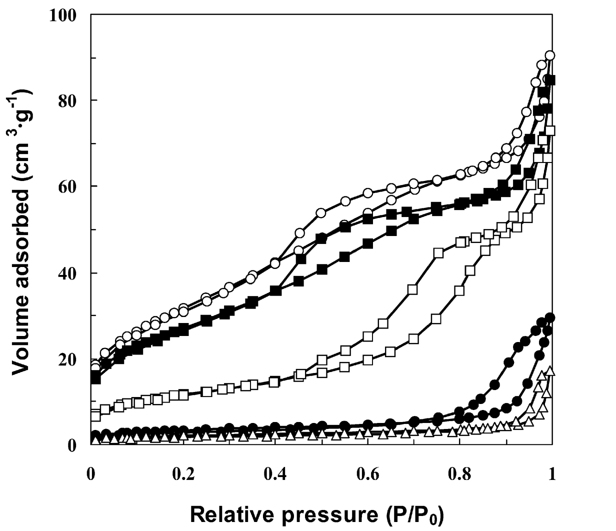

Fig. 2. Nitrogen physisorption isotherms of Nb_2O_5 calcined at (○) 350, (■) 400, (□) 500, (●) 600, and (△) 700 °C.

Table 1
Texture properties of calcined Nb_2O_5 catalysts

Calcination temperature (°C)	BET surface area ($m^2\,g^{-1}$)	Pore volume[a] ($cm^3\,g^{-1}$)	Average pore diameter (nm)	
			BJH adsorption	BJH desorption
350	115	0.14	5.1	4.7
400	99	0.13	5.6	5.0
500	42	0.11	10.3	8.0
600	12	0.05	21.1	16.6
700	7	0.03	20.7	22.0

[a] Measured at $P/P_0 = 0.995$.

volume (from 0.14 to 0.03 $cm^3\,g^{-1}$), which were especially remarkable when the calcination was done at temperatures above 400 °C. The average pore diameter, ca. 5 nm for the samples calcined at 350 and 400 °C, also increased remarkably after calcination at 500–700 °C. The surface area data agree well with those reported by Tanabe et al. [23], whose data were 126 $m^2\,g^{-1}$ after the evacuation at 300 °C and 42 $m^2\,g^{-1}$ after evacuation at 500 °C.

3.2. *TG-DTA and XRD*

Fig. 3 shows the (A) TG-DTG and (B) DTA curves of the $Nb_2O_5 \cdot nH_2O$ precursor. The weight loss on the TG curve closely matched the endothermic feature on the DTA curve, which should suggest an endothermic dehydration process. Most of the crystallization water in the hydrated precursor was removed by heating up to 350 °C; the H_2O/Nb_2O_5 ratio was ca. 3.3 (molar) according to the TG-DTG measurement (Fig. 3A).

The DTA curve also showed a sharp exothermic peak at ca. 585 °C (Fig. 3B). This exothermic feature, which is similar to the one at ca. 570 °C in the earlier report of Tanabe et al. [23], characterizes a transformation of the sample from its amorphous state to crystalline Nb_2O_5.

Fig. 4 shows the effect of calcination temperature on the XRD patterns of Nb_2O_5 catalysts. The samples calcined at 350 and 400 °C appeared as amorphous materials, with no distinct

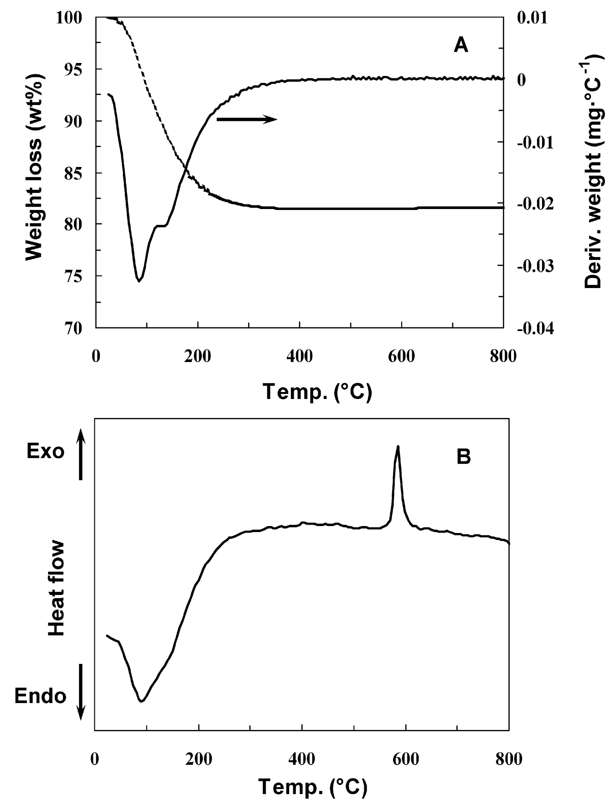

Fig. 3. (A) TG-DTG and (B) DTA curves of the hydrated niobium oxide.

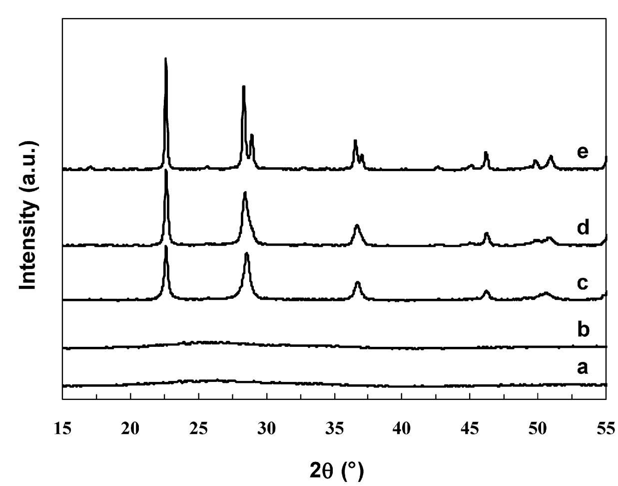

Fig. 4. XRD patterns of Nb_2O_5 samples calcined at (a) 350, (b) 400, (c) 500, (d) 600, and (e) 700 °C.

X-ray diffraction detected with these two samples. Clear diffractions at $2\theta = 22.6°$, $28.4°$, $36.7°$, and $46.2°$ for pseudo-hexagonal Nb_2O_5 crystals (TT phase) [17] appeared for the samples calcined at 500 and 600 °C. The peaks at $2\theta = 28.4°$ and $36.7°$ were found to split into two peaks when the calcination temperature was increased to 700 °C. This splitting indicates a transformation of the pseudohexagonal TT phase to the orthorhombic phase (T phase) of Nb_2O_5 during the calcination at 700 °C [17]. The pseudohexagonal TT phase has a lower crystallinity and can be considered a modification of the orthorhombic T phase [17].

3.3. Catalyst acidity

Based on their acid strength, acid sites at the catalyst surface are divided into the following three groups: medium-strong and weak ($-3.0 \leqslant H_0 \leqslant 6.8$), strong ($-8.2 \leqslant H_0 \leqslant -3.0$), and very strong ($H_0 \leqslant -8.2$). The total amount of acid sites in the three groups is defined as the total acidity ($H_0 \leqslant 6.8$). Fig. 5 shows the effect of calcination temperature on the acidity and acid site distribution of the Nb_2O_5 catalysts. The highest acid strength of Nb_2O_5 samples decreased with increasing calcination temperature (T): $H_0 \leqslant -8.2$ for $T = 350\,°C$, $-8.2 \leqslant H_0 \leqslant -3.0$ for $T = 400$–$600\,°C$, and $-3.0 \leqslant H_0 \leqslant 6.8$ for $T = 700\,°C$. The increase in the calcination temperature also reduced the catalyst acidity (amounts) in the different acid strength ranges. These acidity data (acid strength and amount) are quite similar to those obtained by Tanabe et al. on Nb_2O_5 samples pretreated/calcined at comparable temperatures [23,24].

Fig. 6 gives the fraction of acid sites with different acid strengths. Very strong acid sites ($H_0 \leqslant -8.2$) were observed only over the sample calcined at 350 °C. The fraction of strong acid sites ($-8.2 \leqslant H_0 \leqslant -3.0$) was as high as 0.6 (i.e., 60% of the total acidity) over the catalyst calcined at 400 °C. The fraction of medium-strong to weak acid sites ($-3.0 \leqslant H_0 \leqslant 6.8$) increased with increasing catalyst calcination temperature.

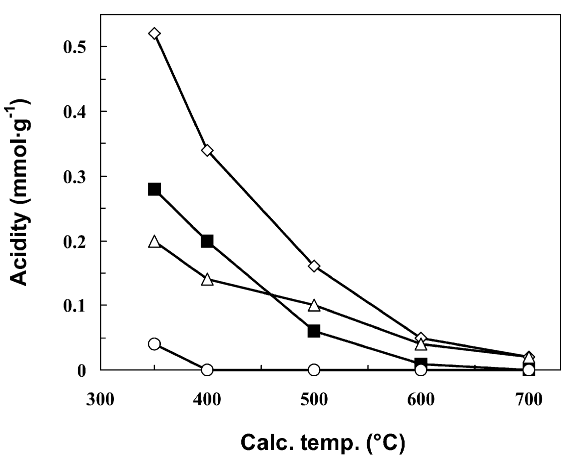

Fig. 5. Effect of the calcination temperature on acidity of Nb_2O_5 samples at (○) $H_0 \leqslant -8.2$, (△) $-3.0 \leqslant H_0 \leqslant 6.8$, and (■) $-8.2 \leqslant H_0 \leqslant -3.0$. The "◇" data give the total acidity at $H_0 \leqslant 6.8$.

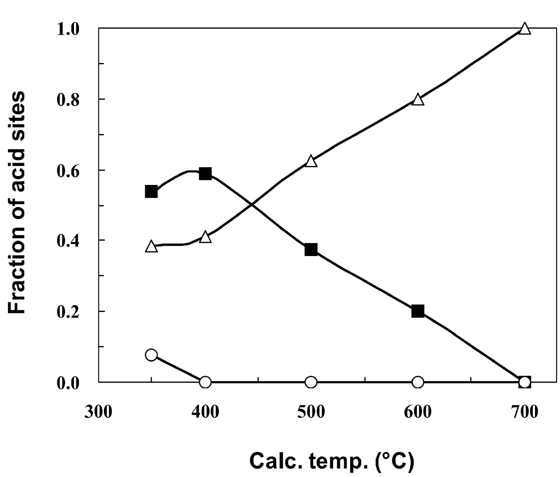

Fig. 6. Effect of the calcination temperature on the fraction of acid sites at (○) $H_0 \leqslant -8.2$, (■) $-8.2 \leqslant H_0 \leqslant -3.0$, and (△) $-3.0 \leqslant H_0 \leqslant 6.8$ over Nb_2O_5 catalyst.

3.4. Catalytic reaction

The catalytic dehydration of glycerol over the present Nb_2O_5 catalysts was characterized by a decrease in the conversion of glycerol with the reaction time on stream (TOS), along with an induction period to reach a stable selectivity for acrolein production. Examples are shown in Fig. 7. With the catalysts calcined at 400 and 700 °C, glycerol conversion decreased with TOS but the selectivity for acrolein increased during the first 3–6 h and stabilized at longer TOS. Thus, catalytic reaction data at TOS of 1–2 and 9–10 h are presented in Fig. 8 to show the effect of calcination temperature on the catalytic performance of Nb_2O_5. The catalyst calcined at 400 °C exhibited the highest selectivity (up to 51 mol% by normalization to glycerol reacted (Fig. 8B)) for acrolein production; despite this, the glycerol conversion based on the catalyst volume (0.63 ml) was slightly lower over this catalyst than over the catalyst calcined at 500 °C (Fig. 8A).

The effect of calcination temperature on the stabilized product distribution (i.e., 9–10 h TOS) is shown in Table 2. In addition to the desirable acrolein, the main product from the

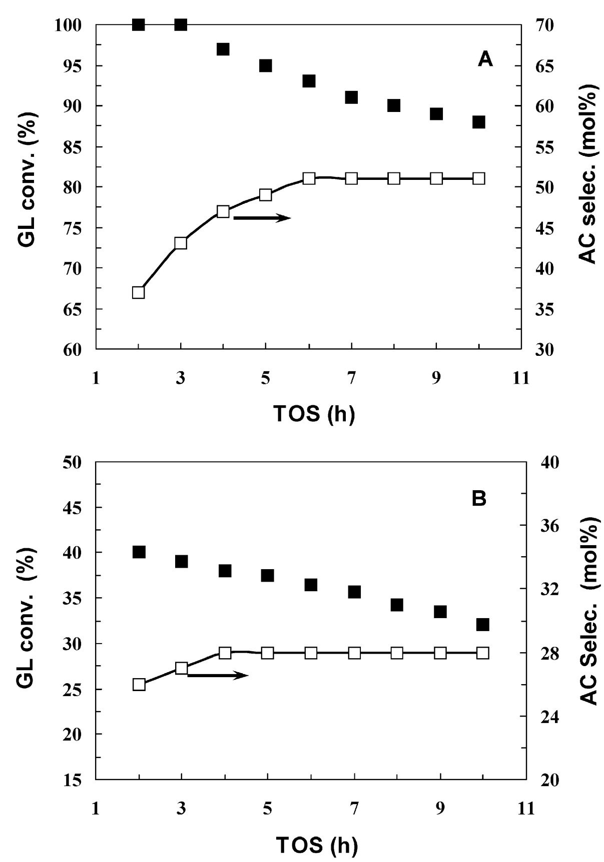

Fig. 7. Time courses of (■) glycerol conversion and (□) acrolein selectivity over Nb_2O_5 catalysts calcined at (A) 400 and (B) 700 °C.

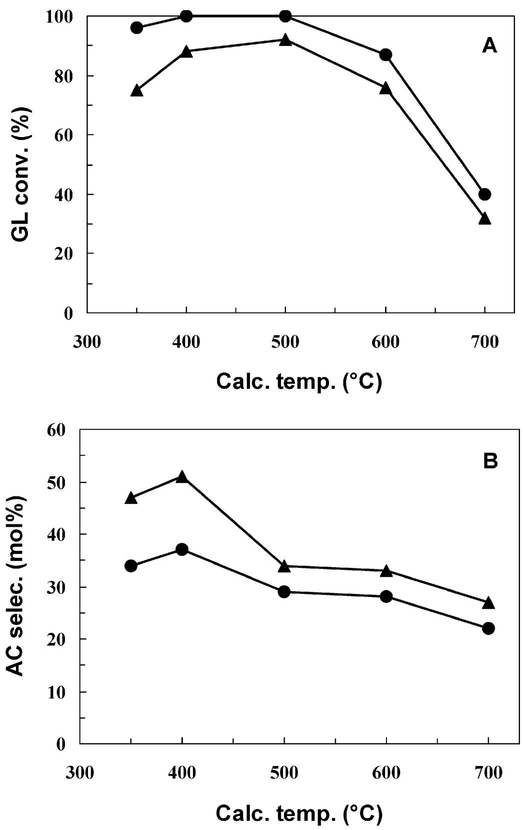

Fig. 8. Effect of the catalyst calcination temperature on (A) glycerol conversion and (B) acrolein selectivity at (●) TOS = 1–2 h and (▲) TOS = 9–10 h.

double dehydration of glycerol, 1-hydroxylacetone from mono dehydration appeared as the main byproduct. The selectivity of 1-hydroxylacetone increased from 10 to 20 mol% with increasing calcination temperature. Other byproducts detected were acetaldehyde, propionaldehyde, acetone, and allyl alcohol, all of which with selectivities usually below 5 mol%. Moreover, quite a large amount of complex compounds (27–45 mol% by normalization to glycerol reacted) remained as unidentified products, possibly formed by secondary reactions among products or between product and the reaction feed. It is noteworthy that the selectivity for unidentified products was the lowest (27 mol%) over the most selective catalyst for acrolein production. In other words, the sample calcined at 400 °C was the best-performing Nb_2O_5 catalyst for the production of acrolein from glycerol.

Attempts were made to regenerate the reacted Nb_2O_5 catalysts by oxidation at elevated temperatures. Whereas recalcination of the used catalyst in flowing air was always effective, a simple oxidation treatment with 20 vol% O_2 in N_2 at the reaction temperature (315 °C) was found to be sufficient for a full regeneration of the reacted Nb_2O_5 catalysts, irrespective of the calcination temperature used in catalyst preparation.

3.4.1. Characterization of carbon deposits

Considerable carbon deposits were formed on the Nb_2O_5 catalysts during the catalytic reaction. TPO characterization of the used catalysts (at 10 h TOS) was conducted using flowing air in the TG-DTA mode; the results are compared in Fig. 9. The weight change below 250 °C on the TG curves (Fig. 9A) was due to the elimination of adsorbed water, because little endothermic features were observed on the corresponding DTA curves (Fig. 9B). The weight loss on the TG curves at 300–500 °C was accompanied by a broad, strong exothermic peak on the DTA curves in the same temperature range, due to burn-off of the carbon deposits by oxidation.

The DTA curves of the used catalysts prepared by calcination at 350 and 400 °C (Fig. 9B) also showed an additional small exothermic peak at ca. 585 °C but with no response on the corresponding TG curves (Fig. 9A). This peak, the position of which closely matched the exothermic feature on the DTA curve of the catalyst precursor (Fig. 3B), indicated a crystallization of the amorphous Nb_2O_5 catalysts (Fig. 4).

The amounts of carbon deposits measured from the TG curves are plotted in Fig. 10 as a function of the catalyst calcination temperature. Whereas the general trend is that catalysts calcined at lower temperatures coked more severely than catalysts calcined at higher temperatures, carbon deposition was significantly heavier on the amorphous catalysts.

We also measured the atomic H/C ratio in the carbon deposits with elemental analysis. The measured H/C ratio appeared to be similar (H/C = 0.50–0.53) for the deposits formed over the catalysts calcined at 400 and 500 °C. Separate XRD characterization of the used catalysts detected no signal for graphitic carbon, suggesting that the carbon deposits existed as amorphous carbon species on the catalyst surface.

4. Discussion

Our data show that Nb_2O_5 catalysts prepared by calcination of a hydrated niobium oxide ($Nb_2O_5{\cdot}nH_2O$) are effective for the gas-phase dehydration of glycerol to produce acrolein. Catalyst performance in the dehydration reaction is significantly affected by the calcination temperature of the Nb_2O_5 catalyst.

Table 2
Effect of calcination temperature on product distribution over Nb_2O_5 catalysts (TOS = 9–10 h)

Calcination temperature (°C)	Conversion (%)	Product selectivity (mol%)						
		Acrolein	Acetaldehyde	Propionaldehyde	Acetone	Allyl alcohol	1-Hydroxylacetone	Others[a]
350	75	47	4.7	2.9	3.1	1.3	10	31.0
400	88	51	4.1	2.4	2.4	1.4	12	26.7
500	92	35	5.3	3.2	3.2	2.3	14	37.0
600	76	33	2.7	1.1	1.1	2.9	21	38.2
700	32	28	1.8	0.4	0.5	5.4	19	44.9

[a] Selectivity for others (mol%) = 100 − total selectivity for all products identified.

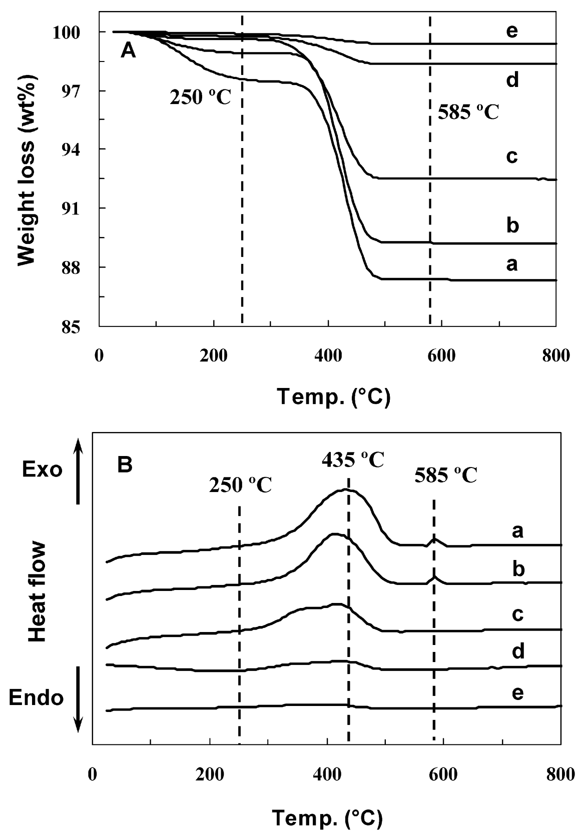

Fig. 9. (A) TG and (B) DTA curves of the used Nb_2O_5 catalysts calcined at (a) 350, (b) 400, (c) 500, (d) 600, and (e) 700 °C.

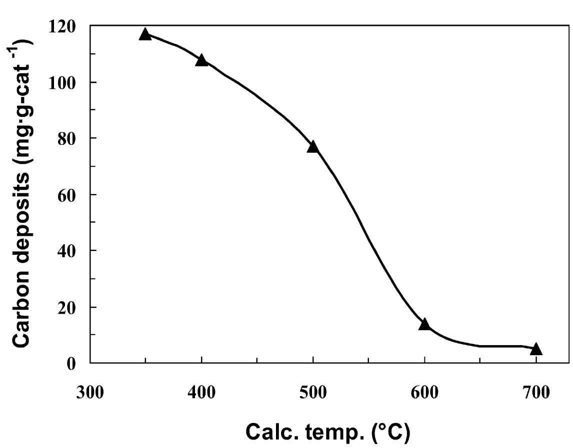

Fig. 10. Effect of the catalyst calcination temperature on the amount of carbon deposits over the used Nb_2O_5 catalysts (TOS = 9–10 h).

Through proper selection of the calcination temperature for catalyst preparation, the desirable acrolein product can be obtained at 315 °C with a stable selectivity >50 mol%.

The catalysts prepared by calcination at 350 and 400 °C were amorphous, as indicated by the TG-DTA and XRD data (Figs. 3 and 4), and also demonstrated the highest surface areas and pore volumes. The catalysts prepared by calcination at higher temperatures (500–700 °C) were crystallized and exhibited quite low surface areas. The amorphous Nb_2O_5 catalysts also showed significantly higher acidity and fractions of strong acid sites in the range of $-8.2 \leqslant H_0 \leqslant -3.0$ compared with the crystallized catalysts (Figs. 5 and 6). These results clearly indicate that the stronger acid sites are reduced more severely than the weaker ones on Nb_2O_5 crystallization during high-temperature calcination. In other words, the amorphous structure seems to be crucial for maintaining a strong acidity of the Nb_2O_5 catalyst [23].

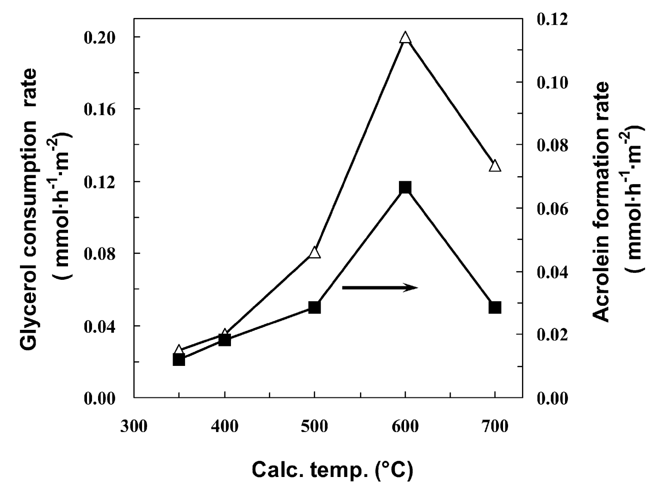

Fig. 11. Areal catalytic rates of Nb_2O_5 catalysts for (△) glycerol consumption and (■) acrolein formation at TOS = 9–10 h.

The reaction data given in Table 2 and Figs. 7 and 8 were based on the catalyst volume (i.e., 0.63 ml) used in our experimental study of the reaction. The areal catalytic rates based on glycerol consumption and acrolein formation at TOS of 9–10 h are shown in Fig. 11. These rates, with distinct maxima on the catalyst calcined at 600 °C, appear to have no clear correlation with catalyst acidity, probably due to a disturbance of the severe catalyst coking. We then made an attempt to normalize the catalytic rates on the catalyst mass. The mass-specific catalytic rates for glycerol consumption and acrolein formation, given in Fig. 12, are better correlated with the fraction of acidity in the range of $-8.2 \leqslant H_0 \leqslant -3.0$ (Fig. 6). Thus, the amorphous catalyst prepared by calcination at 400 °C exhibited the highest efficiency for acrolein production in the dehydration of glycerol, which means that the strong acid sites at $-8.2 \leqslant H_0 \leqslant -3.0$ more effectively catalyzed the selective dehydration of glycerol for acrolein production compared with the stronger ($H_0 \leqslant -8.2$) or weaker acid sites ($-3.0 \leqslant H_0 \leqslant 6.8$). The strong acid sites of $-8.2 \leqslant H_0 \leqslant -3.0$ on supported H_3PO_4 catalysts have been claimed to be effective acid sites for the same reaction in a U.S. patent [10].

The foregoing discussion does not contain any information on the dependence of acrolein production on the nature of acid sites, because the amine titration acidity using Hammett indicators can not distinguish Brønsted and Lewis acid sites. IR spectra of pyridine adsorbed on Nb_2O_5 samples pretreated/evacuated at 100–500 °C were measured by Tanabe et al. [23]. Brønsted as well as Lewis acid sites were detected over the samples evacuated at temperatures below 500 °C. The absorption associated with Brønsted acid sites (ca. 1540 cm^{-1}) appeared to decrease remarkably with increasing evacuation temperature and became invisible when the evacuation was done at 500 °C. The absorption associated with Lewis acid sites

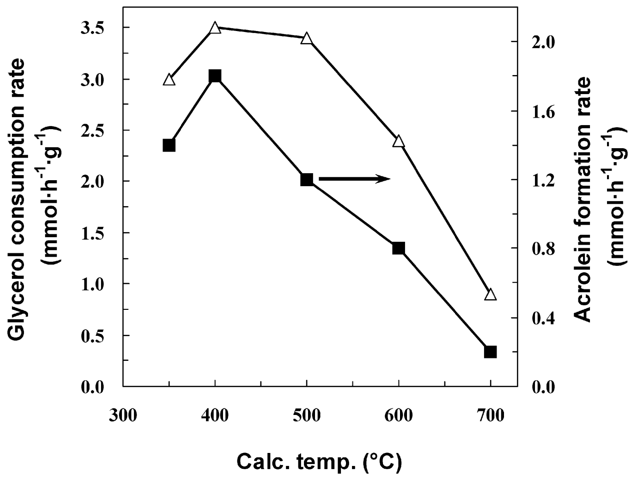

Fig. 12. Mass specific catalytic rates of Nb_2O_5 catalysts for (△) glycerol consumption and (■) acrolein formation at TOS = 9–10 h.

(1446–1448 cm^{-1}) was still distinct on the sample pretreated at 500 °C, however. The ratio of Brønsted to Lewis acid sites (B/L), defined as the intensity ratio of the IR absorption band at ca. 1540 cm^{-1} (Brønsted) to that at 1446–1448 cm^{-1} (Lewis), decreased with increasing evacuation temperature [23]. The information is applicable to our study because the surface area, XRD, and *n*-butylamine titration data of our samples (Table 1, Figs. 3 and 5) were similar to those of Tanabe et al. on the samples subjected to similar pretreatments [19,23,24].

Thus, the percentage of Brønsted acid sites at the surface of the amorphous Nb_2O_5 samples obtained by calcination at 350 and 400 °C in the present study was higher than that at the surface of the crystallized samples prepared at higher calcination temperatures. The better catalytic performance of these amorphous Nb_2O_5 catalysts could imply that Brønsted acid sites can be advantageous over Lewis acid sites for acrolein production from glycerol dehydration. However, this point remains to be confirmed with in situ discrimination of the active acid sites in the dehydration reaction, because the assessment of Brønsted and Lewis acid sites was based on well-dehydrated Nb_2O_5 samples [23]. It is not impossible that under the reaction conditions, some percentage of the Lewis acid sites on the calcined/dehydrated Nb_2O_5 catalysts could be converted to Brønsted ones by reaction with H_2O molecules [25], because the dehydration reaction of glycerol in the present study was conducted in the presence of a large excess of H_2O molecules (a molar water/glycerol ratio of 9!). According to Tanabe et al. [23], Brønsted acid sites of niobic acid or hydrated niobium oxide are much more active than Lewis acid sites for the isomerization of 1-butene, but those Brønsted acid sites eliminated by evacuation at 300 °C can be quantitatively regenerated with suitable rehydration. However, the regeneration of Brønsted acid sites becomes impossible once the evacuation temperature is increased to 500 °C. Tanabe et al. [23] explained the irreversible loss of Brønsted acid sites by the irreversible formation of the TT phase during the high-temperature (500 °C) treatment. Nevertheless, our present data show that Brønsted acid sites can be superior to Lewis acid sites for the formation of acrolein in the dehydration of glycerol over Nb_2O_5 catalysts. This conclusion is further supported by our investigation of the dependence of acrolein production on catalyst acid–base properties over a wide variety of solid acids and bases [27].

The amorphous carbon deposits formed on Nb_2O_5 catalysts could result from consecutive reactions of the products or side reactions between the reactant with such product molecules as acrolein, acetaldehyde, propionaldehyde, and 1-hydroxylacetone, and unidentified byproducts as well [27]. The quite low atomic H/C ratios (H/C = 0.50–0.53) from our elemental analysis of the coked Nb_2O_5 catalysts suggest that the carbon deposits are polyaromatic-like surface species [26]. This seems quite unusual because in the transformation of hydrocarbons over solid acid catalysts, polyaromatic carbon deposits with similar H/C ratios are usually formed in pseudographitic phase at much higher temperatures (above 420 °C) [26]. Nevertheless, it is noteworthy that a simple switch of the coked Nb_2O_5 catalysts to a flow of 20 vol% O_2/N_2 at the reaction temperature (315 °C) was sufficient for a full regeneration of the deactivated Nb_2O_5 catalysts. This property could be important from the standpoint of potential applications.

5. Conclusion

Our findings demonstrate that Nb_2O_5 catalysts prepared by calcination of hydrated niobium oxide are effective for the gas-phase dehydration of glycerol to produce acrolein. The catalyst performance for the dehydration reaction is significantly affected by the catalyst calcination temperature that induces the changes in surface acidity and crystallization of Nb_2O_5. The calcinations at 350 and 400 °C produce amorphous Nb_2O_5 catalysts that exhibit significantly higher acidity and fraction of strong acid sites at $-8.2 \leqslant H_0 \leqslant -3.0$ compared with the crystallized Nb_2O_5 samples obtained by calcination at 500–700 °C. The amorphous catalyst calcined at 400 °C shows the highest fraction of acid sites at $-8.2 \leqslant H_0 \leqslant -3.0$ and gives the highest catalytic efficiency for the formation of acrolein. Deactivation was observed for all of the Nb_2O_5 catalysts, but a simple treatment with flowing air at the reaction temperature was found to be sufficient to regenerate the deactivated catalysts to their original activity.

Acknowledgments

We thank CBMM (Brazil) for kindly providing us with the $Nb_2O_5 \cdot nH_2O$ (HY 340) sample. This work was partly supported by NSF China (Grant 20590362).

References

[1] D.L. Klass, Biomass for Renewable Energy, Fuels and Chemicals, Academic Press, San Diego, 1998, p. 1.
[2] G. Centi, S. Perathoner, Catal. Today 77 (2003) 287.
[3] H. Van Bekkum, P. Gallezot, Top. Catal. 27 (2004) 1.
[4] G.W. Huber, J.A. Dumesic, Catal. Today 111 (2006) 119.
[5] I. Diaz, C. Marquez-Alvarez, F. Mohino, J. Perez-Pariente, E. Sastre, J. Catal. 193 (2000) 295.
[6] T. Miyazawa, Y. Kusunoki, K. Kunimori, K. Tomishige, J. Catal. 240 (2006) 213.
[7] J.M. Clacens, Y. Pouilloux, J. Barrault, Appl. Catal. A 227 (2002) 181.

[8] T. Hass, A. Neher, D. Arntz, U.S. patent 5 426 249, 1995, to Degussa Aktiengesellschaft.
[9] H. Adkins, W.H. Hartung, Org. Synth. Coll. 1 (1941) 15.
[10] A. Neher, T. Haas, D. Arntz, H. Klenk, W. Girke, U.S. patent 5 387 720, 1995, to Degussa Aktiengesellschaft.
[11] E. Schwenk, M. Gehrke, F. Aichner, U.S. patent 1 916 743, 1933, to Scheering-Kahlbaum.
[12] S. Ramayya, A. Brittain, C. DeAlmeida, W. Mok, M.J. Antal, Fuel 66 (1987) 1364.
[13] M.J. Antal Jr., W.S.L. Mok, G.N. Richards, Carbohydr. Res. 199 (1990) 111.
[14] L. Ott, M. Bicker, H. Vogel, Green Chem. 8 (2006) 214.
[15] K. Tanabe, CHEMTECH 21 (1991) 628.
[16] K. Tanabe, S. Okazaki, Appl. Catal. A 133 (1995) 191.
[17] I. Nowak, M. Ziolek, Chem. Rev. 99 (1999) 3603.
[18] K. Tanabe, Catal. Today 78 (2003) 65.
[19] K. Tanabe, M. Misono, Y. Ono, H. Hattori, New Solid Acids and Bases: Their Catalytic Properties, Elsevier, Amsterdam, 1989, pp. 5 and 61.
[20] H.A. Benesi, J. Am. Chem. Soc. 78 (1956) 5490.
[21] H.A. Benesi, J. Phys. Chem. 61 (1957) 970.
[22] K.S.W. Sing, D.H. Everett, R.A.W. Haul, L. Moscou, R.A. Pierotti, J. Rouquerol, T. Siemieniewska, Pure Appl. Chem. 57 (1985) 603.
[23] T. Iizuka, K. Ogasawara, K. Tanabe, Bull. Chem. Soc. Jpn. 56 (1983) 2927.
[24] Z.-H. Chen, T. Iizuka, K. Tanabe, Chem. Lett. 13 (1984) 1085.
[25] M. Craus, in: G. Ertl, H. Knözinger, J. Weitkamp (Eds.), Handbook of Heterogeneous Catalysis, vol. 5, VCH, Weinheim, 1997, p. 2370.
[26] M. Guisnet, in: G. Ertl, H. Knözinger, J. Weitkamp (Eds.), Handbook of Heterogeneous Catalysis, vol. 2, VCH, Weinheim, 1997, p. 626.
[27] S.-H. Chai, H.-P. Wang, Y. Liang, B.-Q. Xu, Green Chem. (2007), doi:10.1039/b702200j, in press.